Rev. Roum. Sci. Techn.– Électrotechn. et Énerg.
Vol. **70**, *3*, pp. 331–336, Bucarest, 2025

SLIDING MODE CONTROLLED CLOSED LOOP QUADRATIC BOOST CONVERTER THREE PHASE INVERTER SYSTEM FED PERMANENT SYNCHRONOUS MOTOR DRIVE WITH ENHANCED RESPONSE

BHAVANI SOMASUNDARAM[1], SIVAPRAKASAM ARUMUGAM[2,*]

Keywords: Quadratic boost converter (QBC); Three phase inverter system (TPIS); Permanent magnet synchronous motor (PMSM); Proportional-integral (PI) and sliding mode (SM) controller.

This research proposes a novel control approach for enhancing the dynamic performance of a quadratic boost converter (QBC) integrated with a three-phase inverter system (TPIS) to drive a permanent magnet synchronous motor (PMSM). The study compares Proportional-Integral (PI) and Sliding Mode (SM) controllers to identify the optimal strategy for achieving fast dynamic response and minimal steady-state error. The SM controller uses a control input derived from analytical torque and stator flux equations to optimize the QBC duty cycle. Simulation results demonstrate superior performance of the SM controller, achieving a settling time of 2seconds and a steady-state speed error of just 1.98 rpm. A PIC16F84-based experimental prototype was developed to validate simulation outcomes. The findings affirm the effectiveness of the SM controller in achieving enhanced speed control and system robustness.

1. INTRODUCTION

Nowadays, PMSM has gained popularity in industrial drives, due to its greater power density, large efficiency and proportionally varying torque to inertia [1,2]. The main objective of drive application is to enhance dynamic response and operate the machine with constant speed loads, which can be achieved through powerful control strategy [3] with high gain converter topology [4-6]. It is highly essential to develop such controllers in order to improve the system's robustness and stability, which is desirable for many drive applications.

Several nonlinear controllers are developed and implemented for improve the dynamic response of the system. From this, the most attracted modified methods were studied and reviewed. The development of PI, FOPID [7], and PR controllers with QBC aims to improve the voltage gain, dynamic response, and stability of PMSM drive systems [8]. The switching table based controller [9-12] is developed to improve the dynamic performance by reducing the torque and flux ripples. Implementation of a PR controller with QBC [13] will enhance the time domain parameters of motor speed even in the application of disturbance. The development of a fuzzy sliding mode controller [14-16] will improve the transient and steady state response of the system. However, the high performance controller can handle PMSM drives effectively and by enhancing the system's robustness.

This work proposes the SM controller with quadratic-BC to modulate the duty cycle of the PWM signal generator through which strengthens the time response of PMSMD. The control input of SM controller constructed using machine equations of PMSM. Further, this paper summarizes the performance results of a proportional integral (PI) and sliding mode controller for QBC based-TPIS fed PMSM drive.

2. MATHEMATICAL MODELING

2.1 PMSM EQUATIONS

In this work, surface-mounted PMSM is used and expressed in the equations (1)-(5)

$$u_d=R_S i_d+L_q i_q P\,\omega+L_d\, di_d/dt. \tag{1}$$

$$u_q=R_S i_q+L_d i_d P\omega+ L_q\, di_q/dt + P\omega\Psi_f. \tag{2}$$

$$T_e= \frac{3}{2}P(\Psi_d i_q - \Psi_q i_d. \tag{3}$$

$$\Psi_d = L_d i_d + \Psi_f. \tag{4}$$

$$J\, d\omega/dt = T_e - T_L. \tag{5}$$

where u_d and u_q are the d and q axis voltages, i_d and i_q are the d and q axis current, L_q and L_d are the q and d axis inductances, Ψ_d and Ψ_q are the d and q axis flux, Ψ_f is the permanent magnet flux, Te is the electromagnetic torque, T_L is the load torque, ω is the motor angular speed, P is the pole pairs, J is the moment of inertia.

2.2 SLIDING MODE (SM) CONTROLLER

The objective is to design a SM controller that drives the motor speed towards the sliding surface and remain in sable. The design of SM controller is based on the Lyapunov stability concept. Taking this function to design the controller is as follows,

$$V = \frac{1}{2}S^2$$

Its derivative is $\dot{V} = S\dot{S} < 0$

The sliding surface S represents the error signal between reference and actual speeds

$$e = \omega_{ref} - \omega = S. \tag{6}$$

$$e = \dot{\omega}_{ref} - \dot{\omega} = \dot{S}. \tag{7}$$

Here e is error signal, ω_{ref} and $\dot{\omega}_{ref}$ are speed and derivative speed reference, S and $\dot{S}$ are sliding and derivative sliding surfaces.

Then, linearized torque derived from eq. (3) and (4), taking$i_d = 0$ becomes

So the equation becomes**,**

$$T_e= \frac{3}{2}P\Psi_f i_q. \tag{8}$$

The derivative speed $\dot{\omega}$ obtained from equations (5) and

[1] Marine Engineering, GKMCET, Chennai-600063, India. E-mail: hodmarine2018@gkmcet.net.in
[2,*] Department of EEE, CEG, Anna University, Chennai-600025, India. E-mail: aspeee@annauniv.edu

DOI: 10.59277/RRST-EE.2025.70.3.8

$$\dot{\omega} = Ai_q - \frac{T_L}{J} \quad (9)$$

where A=3/2* P/J* Ψ_f and T_L/J is load disturbance

Substituting expression $\dot{\omega}$ in equation (8) gives,

$$\dot{S} = \dot{\omega}_{ref} - Ai_q + T_L/J \quad (10)$$

Choosing the reaching law (W.Gao et al.,1993)

$$\dot{S} = \rho sign(s) \quad (11)$$

Equating (10) and (11), the proposed control input is designed as follows

$$i_q = 1/A\,(\dot{\omega}_{ref} + T_L/J + \rho sign(s)) \quad (12)$$

Here, $\rho > 0$

$\rho sign(s)$ is switching law, which forces the speed error to reach switching manifold and it satisfies the derivative condition $\dot{V} < 0$.

The proposed control input is i_q continuous and lies in the range of $0<i_q<1$. It improves the QBC voltage by which steady state error of the speed is reduced.

3. SYSTEM DESCRIPTION

Block diagram of the PI controlled QBC-TPIS fed PMSM drive is delineated in Fig. 1. Step rise is considered in input voltage. The motor's speed is measured and compared with the reference speed. The difference in the speed is processed through PI controller1 and torque reference generated. The difference in torque error is obtained by comparing reference torque and actual torque of the motor. The torque difference is fed to control the pulse width of the PWM signal generator through torque PI controller and the speed regulation is performed.

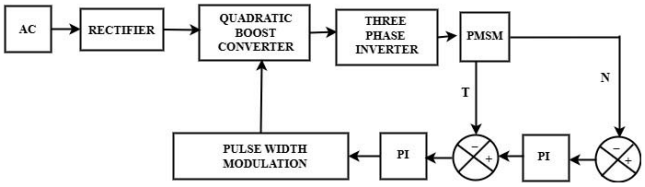

Fig. 1 – Block diagram of PI-QBC-TPIS-PMSM drive.

Block diagram of the SM controlled-QBC-TPIS fed PMSM drive is delineated in Fig. 2. The motor's speed is recorded and compared with the reference speed. The difference in the speed is fed back from the sensing circuit to control the pulse width of the PWM signal generator through which the speed regulation is performed.

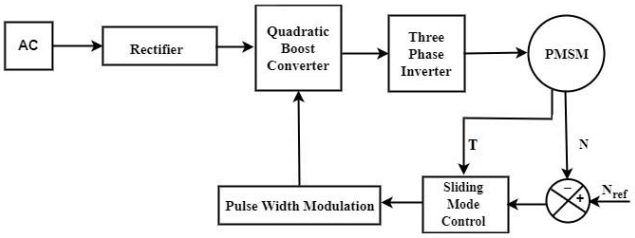

Fig. 2 – Block diagram of SMC-QBC-TPIS-PMSM drive.

The SM controller employs the switching law, which is more likely to enhance the drive's performance, in place of the PI controller's proportional and integral gain (kp, ki).

4. SIMULATION RESULTS

Based on the derived equation, a closed loop QBC-TPIS fed PMSM with SM controller is designed in MALAB environment as delineated in Fig. 4. The SM controller is replaced with PI-PI controller and illustrated in Fig. 3.

Figure 5 shows that a sudden change in input voltage is applied to rectifier at 1s, which is 220 V. The QBC's output voltage both with and without a PI-PI and SM controller are recorded and illustrated in Fig.6. The graph shows that, in the absence of a controller, the QBC has stepped up the voltage from 420V to 480V.

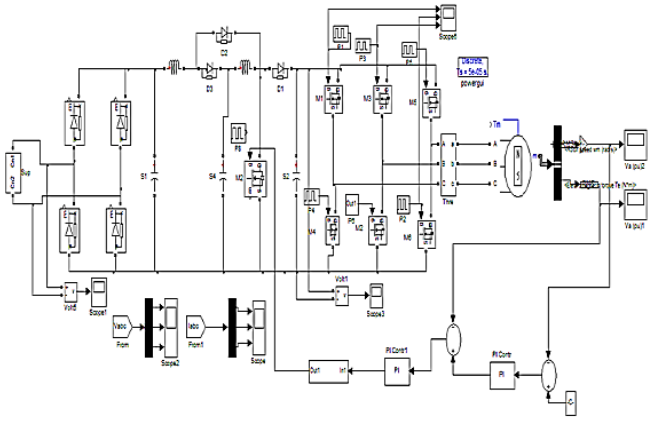

Fig. 3 – Circuit diagram of closed loop QBC -TPIS fed PMSM with PI.

This open loop unregulated voltage is regulated by introducing the controller.

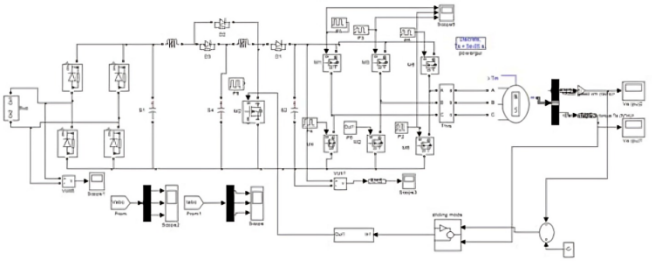

Fig. 4 – Closed loop QBC-TPIS fed PMSM with SM controller.

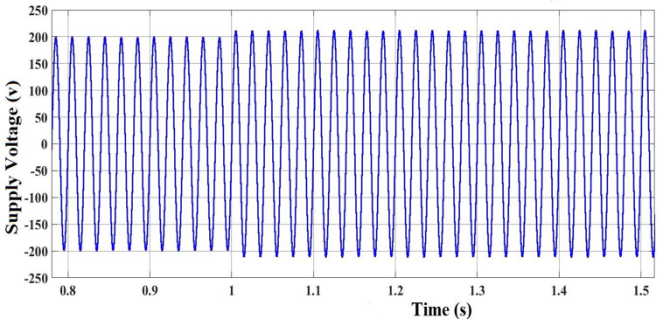

Fig. 5 –Input voltage.

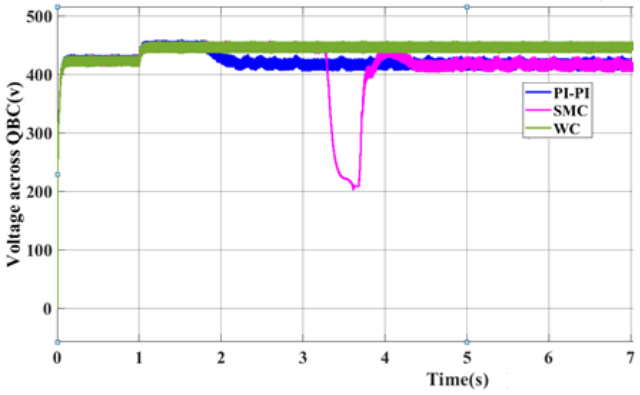

Fig. 6 – Voltage across QBC with PI-PI, SM and without controller.

Through the application of PI-PI, voltage across QBC, initially decreases and then settled to 420 V. Due to PI control action it responds more gradually to changes, leading to larger settling time. In particular, the SM controller's strategy is faster and more robust in rejecting change in supply voltage, along with exhibiting higher control efforts during transients, leading to the voltage over QBC rising initially and settling at 420 V. The effectiveness of QBC-SM controller can be clearly seen in Fig. 7.

Notably, a motor speed variation without a controller is oscillated and increases from 1400 rpm to 1500 rpm. From the speed graph, after transition of change in input voltage the peak speed at undershoot is 250 rpm for PI controller, while 60 rpm for SM controller. Due to the reaching law of SM, it smoothly reaches steady speed of 1400rpm with less time to convergence of speed error compared to PI controller.

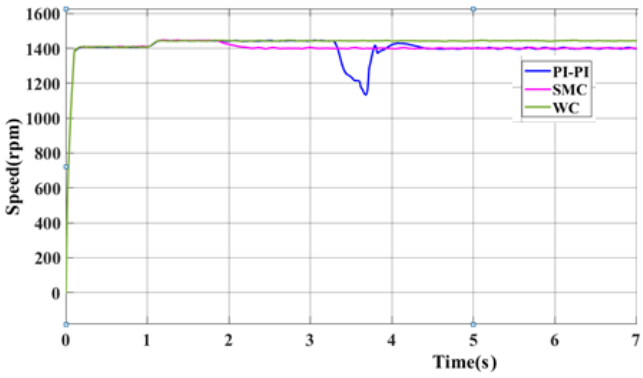

Fig. 7 – Motor speed with PI-PI, SM and Without controller.

Figure 8 shows that the relationship between the output torque fluctuation and its similar trend to the motor speed when the supply is increased. It is found that SM controlled-CL-QBC-TPIS-PMSMD has a very smooth speed and torque response.

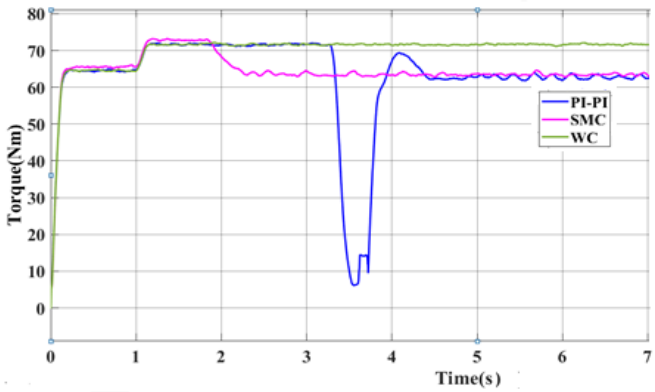

Fig. 8 –Motor torque with PI-PI, SM and Without Controller

Due to the derived control input of the SM controller, this tunes the pulse width, the speed and torque rise and decreases to the specified value. The SM controller is self-assertive and compensates faster by initially increasing the control parameter such as voltage, speed and torque to bring PMSM drive back to the steady state quickly.

4. COMPARISON STUDY

To justify the superiority of the Controller, quantitative assessment of different reference speed values are executed between PI-PI and SM Controller. Particularly, the SM controller come up with enhanced response followed derived control input for necessary modulation.

Table 1

Comparison of time domain parameters at various speeds

Reference speed (rpm)	Type of controller	Tr (s)	Tp (s)	Ts (s)	Ess (rpm)
1450	PI	1.1	3.74	6.36	6.20
	SMC	1.08	1.78	2.20	2.29
1475	PI	1.17	3.70	5.86	5.93
	SMC	1.07	1.71	2.15	2.23
1400	PI	1.12	3.62	4.38	5.56
	SMC	1.06	1.65	2.00	1.98

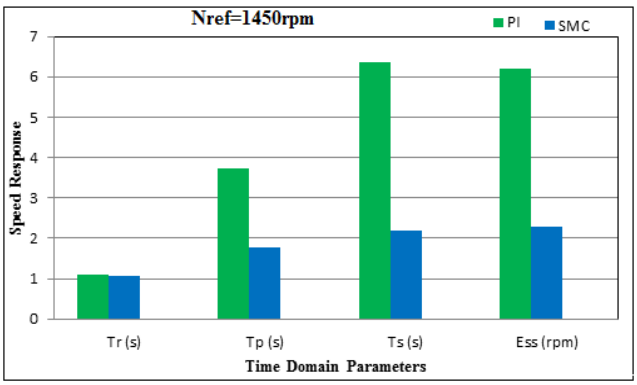

Fig. 9 – Bar chart representation of time domain parameters Nref-1450rpm

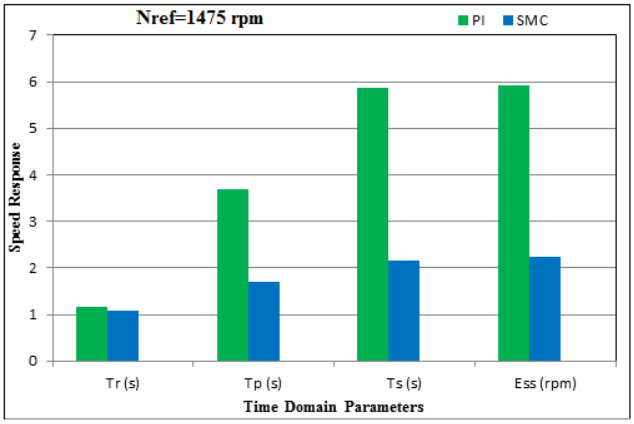

Fig. 10 – Bar chart representation of time domain parameters Nref-1475 rpm.

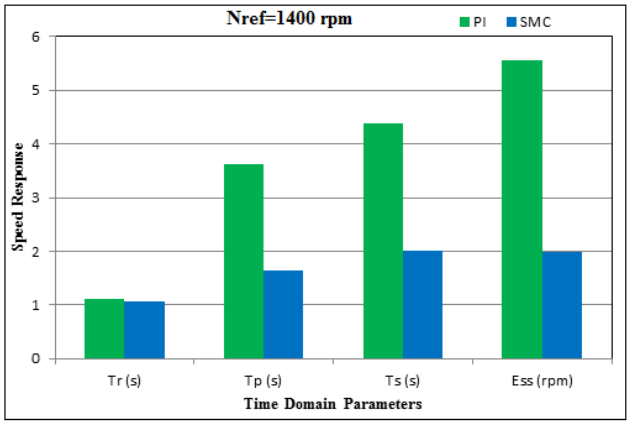

Fig. 11 – Bar graph representation of time domain parameters Nref-1400 rpm.

The comparison study with time domain parameters values are demarcated in Table 1. It is clear from Table 1 that the time response is enhanced in the SM controller compared to the PI controller. From the table, at the reference speed 1450 rpm, the SM controller's rise time is shortened from 1.1s to 1.08 s, peak time notably decreased from 3.74 s to 1.78 s, the duration of settling is abridged from 6.36 s to 2.20 s and steady state error is reduced from 6.20 rpm to 2.29 rpm. Similarly, the reference speeds of 1475 rpm and 1400 rpm are illustrated in table. Bar graph representation of time domain specifications with different reference speeds are demarcated in Fig. 9, 10 and 11.

The quantitative comparison of simulated and hardware outcomes are presented in Table 2. The simulated input voltage, switching frequency and inverter output voltage are closely connected to the hardware results with low percentage error of 1.19 %. Due to the voltage drop in chokes and devices, the inverter output voltage of hardware has fewer drops than the simulated voltage.

Table 2

Simulation outcome compared with hardware outcome

Parameter	Simulation Result	Hardware Result
Input voltage	200V	200 V
Switching frequency of QBC	5kHz	5kHz
Switching frequency of three phase inverter	10Hz – 100Hz	10Hz – 100Hz
Inverter output voltage	420V	415V

On comparing all the inferences, it can be concluded that SM controlled-CL-QBC-TPIS provides better control considering the simulated outcomes of sudden change in supply voltage, Voltage across Quadratic Boost (QB) Converter, motor speed and torque. Consequently, the SM controlled-CL-QBC-TPIS is suggested for constant load application due to its robustness against source variation.

6. EXPERIMENTAL RESULTS

Figure 12 demonstrates the hardware snapshot for the SC-QBC-TPIS- fed PMSM drive system. The hardware resides with the rectifier unit, QBC, transformer, driver unit (IR2110), three-phase inverter system (TPIS), and motor load.

The working procedure of the board started from the transformer (T/F), which supplies alternating current to single phase diode bridge rectifier. The PIC 16F8C microcontroller generates pulses to the MOSFET switch of the QBC and the inverter system.

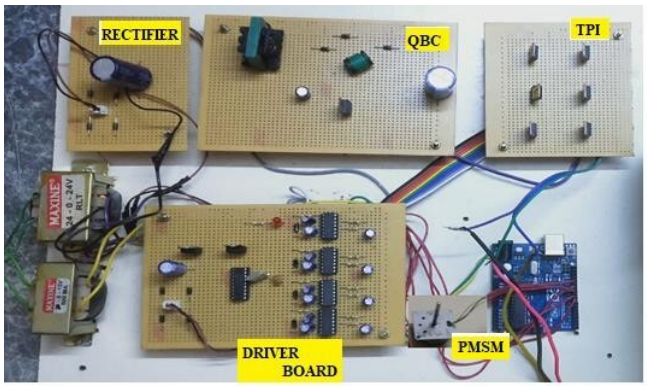

Fig. 12 – Hardware snapshot of VSI-PMSM.

The experimental outputs of model were recorded using CRO. The QBC switching pulse S1, QBC output voltage, PMSM's load voltage and PMSM's load current are illustrated in Fig .13.

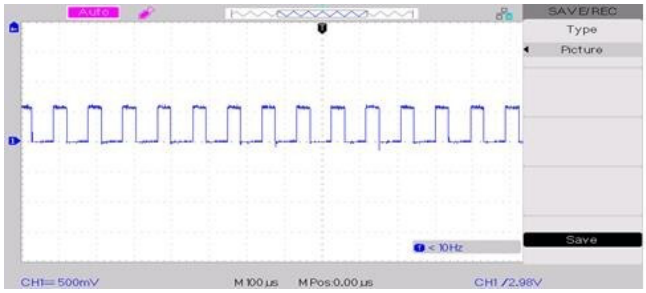

Fig. 13a – QBC switching pulse S1.

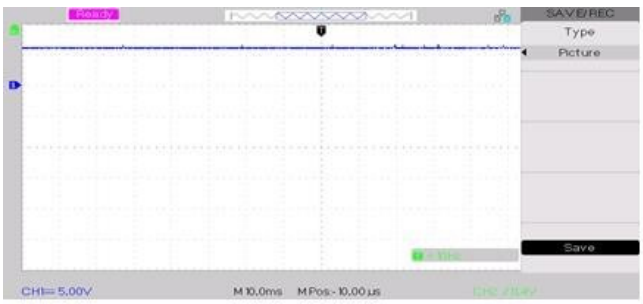

Fig. 13b – QBC output voltage.

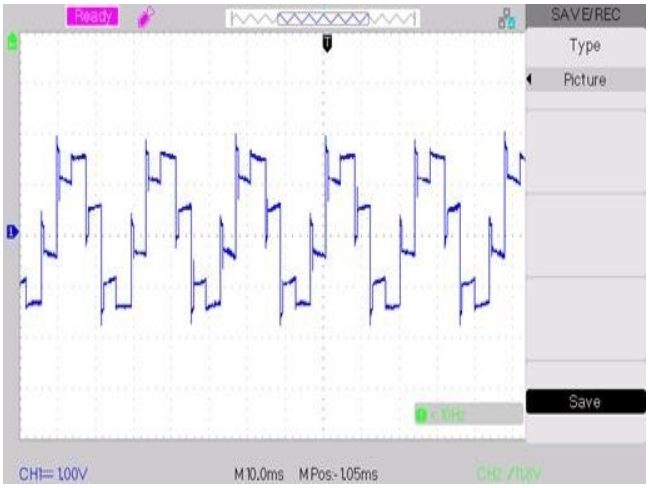

Fig. 13c – Motor's load voltage.

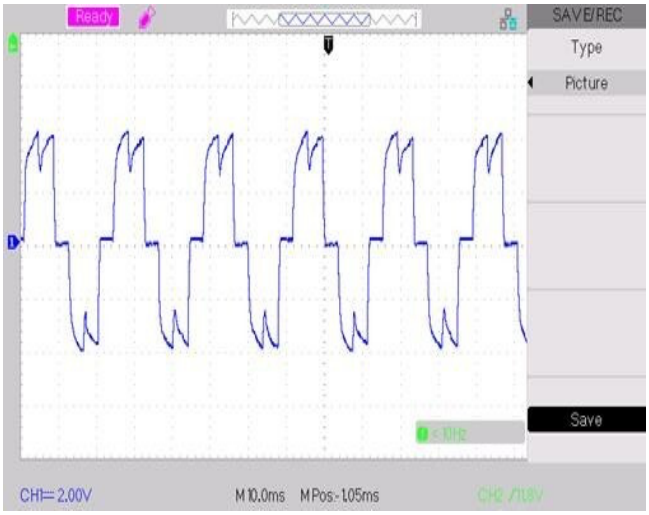

Fig. 13d – Motor's load current of TPIS-PMSM system.

The control board contains a PIC microcontroller and four driver ICs, where three drivers drive the three legs of the inverter, and one driver triggers the MOSFET of QBC. Here, the PMSM acts as a load, and the results are taken.

The outcome of hardware shows that the QBC equipped with the QBC-TPIS-PMSM system provides an increase in output voltage by the duty ratio times the switch. Hence, the built structure of the QBC prototype model delivers suitable performance to the drive application.

7. **CONCLUSIONS**

In this work, PI and SM controlled the CL-QBC-TPIS-PMSMD system has been designed and simulated. Improving the PMSMD system's time responsiveness is the primary goal of the work. Through the variation in input voltage, the strength of the CL-QBC-TPIS-PMSMD is enhanced, and the proposed control input maintains the speed and torque at their actual values. It is notable that a balanced output voltage is achieved via QBC with an upgraded control signal at the controller's control input. A specific analysis is performed between the two controllers, and the outcomes are evaluated in terms of settling time and steady-state error. By utilizing the SM controller, the rise time and peak time are reduced to 1.06 s and 1.65s; the settling time is settled at 2s; the Steady state error is less than 1.98 rpm. Hence, the result of the work shows that the SM controller is superior to the PI-controlled PMSM drive. Further, the hardware setup demonstrates enhanced parameters in the control strategy, including the QBC switching pulse S1, QBC output voltage, voltage across the motor, and current through the motor load.

The present work deals with the development of closed loop PMSM drive with SM Controller. CL-QBC-TPIS fed PMSM with FLC will be implemented in future. Also, the multiple disturbance investigations for SC-QBC-TPIS are possible. The hardware model of SC-QBC-TPIS will be implemented for higher power levels.

ACKNOWLEDGEMENTS

The author wants to thank the supervisor for his guidance and constant support

CREDIT AUTHORSHIP CONTRIBUTION STATEMENT

Bhavani Somasundaram: Preparing manuscript, simulation.
Sivaprakasam Arumugam|: Output discussions, correcting manuscript, and review.

Received on 22 August 2024

REFERENCES

1. R. Krishnan, A.J. Beutler, *Performance and design of an axial field PM synchronous motor servo drive*, in Conf. Rec. IEEE-IAS Annul. Meeting, pp. 634–640 (1985)
2. P. Pillay, *Application characteristics of permanent magnet synchronous and brushless DC motors for servo drives*, IEEE Transactions on Industry Applications, **21**, *5,* pp.986–996 (1991)
3. E. Sreeshobha, G. Sree Lakshmi, *Performance analysis and comparison of P.I. controller and ANN controller of bidirectional DC/DC converter for hybrid electric vehicle system*, 2022 International Conference on Breakthrough in Heuristics and Reciprocation of Advanced Technologies (BHARAT), Visakhapatnam, India (2022).
4. S. Li, W. Xie, K. Ma-Smedley, *A family of an automatic interleaved Dickson switched-capacitor converter and its ZVS resonant configuration*, IEEE Trans. Ind. Electron. **66**, *11*, pp. 255-264 (2019).
5. C.Y Chan**,** *An improved voltage-mode controller for the quadratic boost converter,* IEEE Transactions on Circuits and Systems II: Express Briefs. **69,** *2*, pp.454-458 (2022).
6. S.H. Chin Cholkar, C.Y Chan, *Design of fixed-frequency pulse width-modulation-based sliding-mode controllers for the quadratic boost converter,* IEEE Transactions on Circuits and Systems II: Express Briefs, **64***, 1,* pp. 2014–2018 (2017).
7. M. Vahedpour, A.R. Noei, H.A. Kholerdi, *Comparison between performance of conventional, fuzzy and fractional order PID controllers in practical speed control of induction motor*, 2015 2nd International Conference on Knowledge-Based Engineering and Innovation (KBEI), Tehran, pp. 912–916 (2015).
8. S. Bhavani, A. Sivaprakasam, *Dual mode symmetrical proportional resonant controlled quadratic boost converter for PMSM- Drive*, Symmetry,**15**,*1*, pp.147 (2023).
9. A. Sivaprakasam, *A new approach to reduce torque ripple and noise in twelve sector based direct torque controller fed permanent magnet synchronous motor drive*: *Simulation and experimental results*, Noise Control Eng. Journal, **65**, *6*, pp .531–548 (2017).
10. A. Sivaprakasam, T. Manigandan, *An alternative scheme to reduce torque ripple and mechanical vibration in direct torque controlled permanent magnet synchronous motor*. Journal of Vibration and Control, **21**, *5*, pp. 855-871 (2013).
11. B. Mokhtari, *Enhancement Ripples of a direct torque control applied to a permanent magnet synchronous motor by using a four-level multicellular inverter and a new reduced switching table*, Rev. Roum. Sci. Techn. – Électrotechn. Et Énerg., **69**, *2*, pp. 207–212 (2024).

12. A. Sivaprakasam, J.D. Anunciya, *A survey on matrix converter-fed direct torque control techniques for AC machines*, IETE Journal of Research, **68**, *1*, pp. 1–17, (2019).
13. S. Bhavani, A. Sivaprakasam, *Hysteretic controlled quadratic boost converter-3 phase inverter fed PMSM for E-car with enhanced time response*, 9th International Conference on Electrical Energy System (ICEES), (2023).
14. A. Mechernene, M. Loucif, M. Zerikat, *Induction motor control based on a fuzzy sliding mode approach.* Rev. Roum. Sci. Techn.– Électrotechn. et Énerg., **64**, *1*, pp.39–44 (2019).
15. R. Rouabhi, A.G. Herizi, S. Djeriou, A. Zemmit, *Hybrid type-1 and 2 fuzzy sliding mode control of the Induction motor,* Rev. Roum. Sci. Techn.– Électrotechn. et Énerg., **69**, *2*, pp.147–152 (2024).
16. W. Gao, J.C. Hung, *Variable structure control of nonlinear systems: a new approach*, IEEE Transactions on Industrial Electronics, **40**, *1*, pp. 45– 55 (1993).